Earthquake (2026) Volume 4 Issue 1 ISSN: 3029-1550 (O)
doi: 10.59429/ear.v4i1.15293

RESEARCH ARTICLE

Geomagnetic Field Variations Associated with Seismic Energy Release: Analysis of Observatory Data from 2021 – 2025

Zukhriddin Shukurov, Valijon Yusupov, Bekruz Shakhriev*

Institute of Seismology of the Academy of Sciences of the Republic of Uzbekistan, Tashkent, Uzbekistan
***Corresponding author:** Valijon Yusupov, Bekruz Shakhriev, valijon.yusupov@mail.ru

ABSTRACT

This study investigates the long-term variations in the mean total geomagnetic field intensity (T, not to be confused with the SI unit tesla) observed during 2021–2025 at the ART and NVS geomagnetic observatories (Russia), IZN (Türkiye), JAI (India), and Yangibozor (YNBZ, Uzbekistan). One-minute geomagnetic observations obtained from the INTERMAGNET database were used to calculate daily and annual mean values. To quantify the annual rate of change of the total field intensity, used here as a proxy for secular variation, a linear regression slope (nT/year) was determined for each observatory and each year. The calculated regression slopes were spatially interpolated using Geographic Information System (GIS) techniques to assess regional variations in the rate of geomagnetic field change. The results revealed spatial differences in regression slope values among the selected observatories, indicating regional differences in the rate of change of the total field. These differences may reflect geodynamo processes in the Earth's outer core, regional geomagnetic characteristics, and the influence of external geomagnetic field sources, which could not be fully separated in this study. In addition, the annual cumulative seismic energy of earthquakes with magnitudes $M \geq 4.0$ occurring within a 200 km radius of each observatory was calculated and compared with the corresponding regression slopes. The results indicate that no consistent linear relationship exists between long-term geomagnetic field variations and annual seismic energy. Similar temporal tendencies were observed at some observatories but not at others, and they do not demonstrate a causal relationship.

Keywords: geomagnetic field; total geomagnetic field intensity; secular variation; regression slope; INTERMAGNET; GIS; seismic energy.

1. Introduction

The Earth's main magnetic field is primarily generated by the geodynamo process, which is driven by the convective motion of electrically conducting molten iron in the outer core. However, geomagnetic observations also contain contributions from magnetized rocks in the lithosphere and external magnetic fields generated by electric currents in the ionosphere and magnetosphere. These contributions vary over different temporal and spatial scales. The gradual change in the Earth's main magnetic field over periods of years and decades is known as secular variation (SV) and primarily reflects dynamic processes occurring

ARTICLE INFO
Received: 11 September 2026| Accepted: 30 October 2026 | Available online: 27 November 2026

CITATION
Shukurov Z, Shakhriev V Y B S, Geomagnetic Field Variations Associated with Seismic Energy Release: Analysis of Observatory Data from 2021-2025. Earthquake. 2026; 4(1): 15293 doi:10.59429/ear.v4i1.15293

COPYRIGHT
Copyright © 2026 by author(s). *Earthquake* is published by Arts and Science Press Pte. Ltd. This is an Open Access article distributed under the terms of the Creative Commons Attribution License (https://creativecommons.org/licenses/by/4.0/), permitting distribution and reproduction in any medium, provided the original work is cited.

within the Earth's outer core. Investigating secular variation is important for understanding core dynamics, improving global geomagnetic field models, and supporting applications in navigation, satellite systems, space weather monitoring, and geophysical exploration [1,4,6]. In practice, observatory records combine the internal secular variation with residual external contributions, a point already emphasised in early analyses of secular variation [26].

Continuous measurements at geomagnetic observatories provide an important basis for investigating long-term changes in the Earth's magnetic field. These observations enable researchers to assess temporal variations in geomagnetic field components, identify regional differences, and evaluate the performance of global geomagnetic models. In addition, satellite missions and the development of Geomagnetic Virtual Observatory (GVO) techniques have expanded opportunities to investigate the spatial and temporal evolution of the geomagnetic field. Magnetic field gradient tensors derived from virtual observatories have also been used to characterize regional features of secular variation and improve the representation of geomagnetic field changes [3–5].

Previous studies have investigated geomagnetic secular variation using different observational and statistical approaches. Wei and Xu examined the westward drift of the Earth's main magnetic field using the International Geomagnetic Reference Field (IGRF) model and discussed its relationship with processes in the outer core [1]. Goguitchaichvili et al. reconstructed the geomagnetic field evolution in Mexico over nearly two centuries using statistical analysis and spline interpolation, identifying long-term variations and geomagnetic jerk events [2]. More recent investigations have demonstrated the importance of combining ground-based observatory measurements with satellite observations to improve geomagnetic field modelling and the assessment of secular variation [4,5].

In addition to studies of long-term geomagnetic field changes, considerable research has addressed possible relationships between geomagnetic variations and seismic activity. Chen et al. investigated changes in geomagnetic transfer functions at the Lunping Geomagnetic Observatory in northern Taiwan and compared them with the cumulative energy released by earthquakes. Their analysis considered earthquakes with magnitudes greater than 4.0 within a 150-km radius of the observatory. The authors examined whether temporal changes in geomagnetic transfer functions were associated with variations in seismic energy release [23]. Mihai et al. investigated geomagnetic variations and seismic energy release in the vicinity of the Vrancea seismic zone, providing another regional assessment of the possible relationship between geomagnetic and seismic processes [24]. Similarly, Yoshino et al. performed a statistical analysis of ultralow-frequency (ULF) geomagnetic signals recorded at the Kakioka Observatory in Japan during 2001–2010. Their results indicated that the occurrence of ULF geomagnetic anomalies varied depending on earthquake energy and epicentral distance [25]. These studies demonstrate the diversity of approaches used to investigate geomagnetic and seismic phenomena. However, the geomagnetic parameters, observation periods, and statistical methods considered in these investigations differ from those applied in the present study.

Despite progress in geomagnetic field modelling and research on seismomagnetic phenomena, further regional investigations are needed to quantify long-term changes in geomagnetic field intensity and compare their temporal and spatial characteristics with regional seismic energy release. In particular, the use of linear regression slopes derived from observatory measurements provides a quantitative measure of the rate of geomagnetic field change. Comparing these slopes among different observatories and mapping their spatial distribution may help identify regional differences in geomagnetic secular variation. Furthermore, comparing annual geomagnetic trends with cumulative seismic energy can provide a preliminary descriptive assessment

of whether similar or contrasting temporal patterns occur in the investigated regions. Such a comparison should not, however, be interpreted as evidence of a direct causal relationship.

In this study, total geomagnetic field intensity (T) measurements recorded during 2021–2025 at five observatories were analysed: ART (Russia), NVS (Russia), IZN (Türkiye), and JAI (India), whose data are associated with the INTERMAGNET network, and Yangibozor (YNBZ, Uzbekistan), whose data were obtained independently from the Yangibozor Geomagnetic Observatory affiliated with the Institute of Seismology of the Academy of Sciences of the Republic of Uzbekistan. Daily mean values were calculated from one-minute geomagnetic observations. Linear regression analysis was then applied to determine the rate of change in total field intensity, expressed as a slope in nT/year, for each observatory and study year. The resulting regression slopes were subsequently used to assess differences in the temporal behaviour of the geomagnetic field among the observatories. Geographic Information System (GIS) techniques were applied to interpolate and map the spatial distribution of the calculated slopes.

Additionally, annual cumulative seismic energy was estimated for earthquakes with magnitudes of $M \geq 4.0$ occurring within a 200-km radius of each observatory. Earthquake information was obtained from the European-Mediterranean Seismological Centre (EMSC), and seismic energy was estimated using the Gutenberg–Richter relationship. The selected magnitude threshold was adopted as an operational criterion for identifying moderate and larger earthquakes in the vicinity of the observatories. Previous research, including that of Chen et al., has also examined geomagnetic variations in relation to earthquakes with magnitudes greater than 4.0, although the spatial selection criteria and analytical approaches differ between studies [23]. The annual cumulative seismic energy was compared with the corresponding geomagnetic regression slopes to examine similarities and differences in their temporal variations.

The primary objective of this study is to quantitatively evaluate changes in total geomagnetic field intensity at five observatories during 2021–2025 using linear regression slopes (nT/year), investigate their spatial distribution through GIS-based mapping, and compare the annual geomagnetic trends with cumulative seismic energy released by nearby earthquakes. By combining geomagnetic observations, regression analysis, spatial interpolation, and seismic energy estimates, this study provides a regional assessment of the annual rate of change of the total geomagnetic field intensity (as a proxy for secular variation) and its possible association with seismic energy release.

2. Materials and Methods

2.1. Geomagnetic Observatory Data

This study analysed the mean total geomagnetic field intensity (T) recorded during 2021–2025 at five geomagnetic observatories located across Eurasia: ART (Arti, Russia), NVS (Novosibirsk, Russia), IZN (Iznik, Türkiye), JAI (Jaipur, India), and YNBZ (Yangibozor, Uzbekistan). Geomagnetic data for the ART, NVS, IZN, and JAI observatories were obtained from the INTERMAGNET database. Data from the Yangibozor (YNBZ) Observatory were obtained directly from the observatory, which is affiliated with the Institute of Seismology of the Academy of Sciences of the Republic of Uzbekistan. Yangibozor is not a member of the INTERMAGNET network; therefore, its data were treated as an independent observational source.

The Yangibozor Geomagnetic Observatory has been operating since 1923 and represents an important source of long-term geomagnetic observations in Central Asia. Geomagnetic field measurements at this observatory are performed using Geometrics G-856 (USA), GSM-19T (Canada), and MV-01 (Russia) proton

magnetometers. According to the available instrument specifications, their sensitivity is approximately 0.1 nT, while the overall measurement uncertainty is reported to be within 0.4–0.6 nT [7].

One-minute geomagnetic observations were used to calculate daily mean values of the total geomagnetic field intensity. For each observatory, the daily mean values were analysed separately for each calendar year from 2021 to 2025. A linear regression model was fitted to the daily mean values within each year to estimate the annual rate of change in the geomagnetic field. The resulting regression slope, converted from nT/day to nT/year (Section 2.4), was used as a quantitative measure of the rate of geomagnetic field variation during the corresponding year. The number of observations (n), the coefficient of determination (R^2), and the p-value were calculated for each regression model to assess the fit of the estimated slope.

The annual regression slopes obtained for the five observatories were subsequently used to examine spatial differences in the rate of geomagnetic field variation. Geographic Information System (GIS) techniques implemented in ArcGIS were applied to interpolate the calculated values and generate annual spatial distribution maps. The geographic coordinates of the selected observatories were used to locate the measurement sites and support the spatial analysis (Table 1 and Figure 1).

To investigate the possible association between geomagnetic field variations and regional seismic activity, earthquakes with magnitudes of $M \geq 4.0$ occurring within a 200-km radius of each observatory were selected. Earthquake information was obtained from the European-Mediterranean Seismological Centre (EMSC). The seismic energy of individual earthquakes was estimated using the Gutenberg–Richter relationship, and the annual cumulative seismic energy was calculated for each observatory region. These annual energy estimates were then compared descriptively with the corresponding geomagnetic regression slopes. This comparison was intended to identify similarities and differences in their temporal variations rather than to establish a direct causal relationship between geomagnetic field changes and seismic activity.

The five observatories were selected to represent different geographic and geomagnetic settings across Eurasia. Their locations in Russia, Türkiye, India, and Uzbekistan provide an opportunity to compare regional differences in the rate of geomagnetic field variation over the 2021–2025 study period. The observatory locations and their geographic coordinates are presented in Table 1 and Figure 1.

Table 1. Geographic information on the locations of the geomagnetic observatories

Observatory	Country	Lat (°N)	Lon (°E)
ART	Russia	56.433	58.567
NVS	Russia	54.850	83.230
YNBZ	Uzbekistan (Tashkent)	41.305	69.574
IZN	Türkiye	40.500	29.720
JAI	India	26.920	75.800

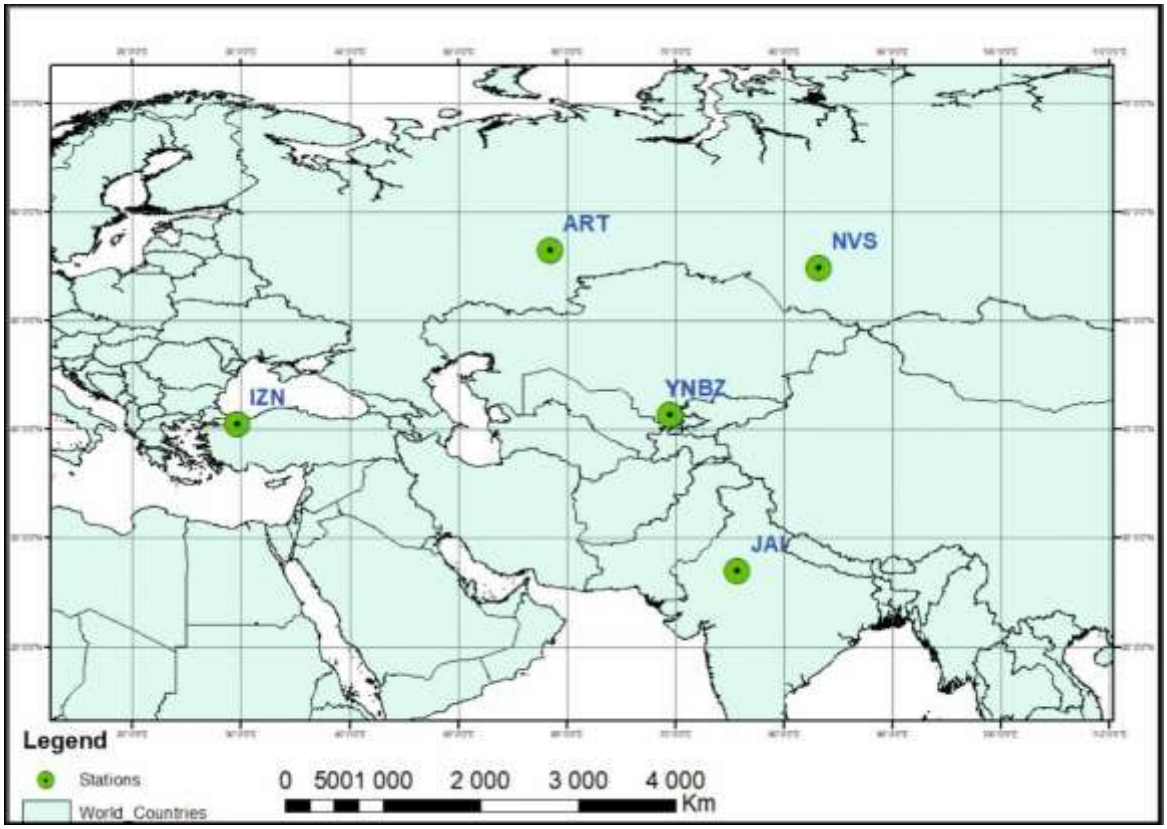

Figure 1. Locations of the five geomagnetic observatories used in this study.

2.2. Geomagnetic Data Sources and Preprocessing

The geomagnetic data used in this study consisted of total field intensity (T) measurements obtained from five observatories located across Eurasia. One-minute geomagnetic observations for the ART (Russia), NVS (Russia), IZN (Türkiye), and JAI (India) observatories were downloaded from the official INTERMAGNET Data Viewer (https://intermagnet.org), which provides standardized geomagnetic observatory data [20]. The Best Available one-minute data product was selected for each observatory.

The data from the Yangibozor (YNBZ) Geomagnetic Observatory in Uzbekistan were obtained directly from the observatory, affiliated with the Institute of Seismology of the Academy of Sciences of the Republic of Uzbekistan. Since Yangibozor is not part of the INTERMAGNET network, its measurements were obtained independently and were not downloaded from the INTERMAGNET Data Viewer.

The analysis covered the period from 1 January 2021 to 31 December 2025. For each observatory, daily mean values of the total geomagnetic field intensity (T) were calculated from the available one-minute observations. Days with missing observations were not artificially reconstructed, and no interpolation was applied to fill data gaps. Consequently, the subsequent regression analysis was based only on available daily mean values.

No additional baseline correction, external field correction, or geomagnetic activity-based filtering was applied to the original observations during the initial data-processing stage. Therefore, the analysed measurements may contain contributions from both internal and external geomagnetic sources, including ionospheric and magnetospheric current systems. This limitation was considered when interpreting the estimated long-term trends.

For each observatory and calendar year, the available daily mean values were used to fit a linear regression model. The resulting regression slope, converted from nT/day to nT/year (Section 2.4), represented the estimated annual rate of change in total geomagnetic field intensity. The number of observations (n), regression slope, coefficient of determination (R^2), and p-value were calculated for each model. These statistical parameters were used to describe the regression results. Only the total intensity T was analysed. The components X, Y and Z were not considered, although $T = \sqrt{(X^2 + Y^2 + Z^2)}$ and therefore $dT/dt = (X \cdot dX/dt + Y \cdot dY/dt + Z \cdot dZ/dt)/T$, so stations with similar dT/dt may differ in the behaviour of their vector components; an analysis of the components is planned.

2.3. Data Processing and Quality Control

The one-minute total geomagnetic field intensity (T) data obtained from the INTERMAGNET Data Viewer were processed using Microsoft Excel. Daily mean values were calculated by averaging the available one-minute observations recorded during each day. These daily mean values were subsequently used as the input dataset for the regression analysis, while annual mean values were calculated to describe the long-term temporal evolution of the geomagnetic field.

The same data-processing procedure was applied to all observatories. Days with missing or incomplete observations were excluded from the analysis, and no interpolation or artificial gap filling was performed. Consequently, the regression analysis was carried out using only the available daily mean values, ensuring methodological consistency and comparability among all observatories.

Geomagnetic field measurements contain contributions from both internal and external sources, including ionospheric and magnetospheric current systems. Although daily and annual averaging can reduce short-term fluctuations, these procedures cannot completely eliminate external geomagnetic contributions. Therefore, the observed long-term variations cannot be attributed exclusively to changes in the Earth's internal magnetic field.

To assess the influence of geomagnetic activity on the regression results, additional sensitivity analyses were conducted using the planetary Kp index obtained from GFZ Potsdam. Three datasets were considered: (i) the complete dataset containing all available daily observations; (ii) a filtered dataset excluding days with a daily maximum Kp index ≥ 5; and (iii) a quiet-day dataset including only days for which all eight 3-hourly Kp values were ≤ 2. The regression results obtained from these datasets were compared with those derived from the complete dataset.

Geomagnetic storm days were retained in the main analysis to preserve the completeness of the observational record and to characterize the overall temporal behavior of the measured total geomagnetic field intensity. The additional Kp-based filtering was performed as a sensitivity analysis to evaluate the extent to which geomagnetic activity may influence the estimated regression trends.

Kp-based filtering does not remove all external-field contributions. In particular, the low-latitude station JAI may be affected by the equatorial electrojet (EEJ), whose influence is not adequately represented by the planetary Kp index. Therefore, the results of the Kp-based analysis should be interpreted as an assessment of sensitivity to geomagnetic activity rather than as a complete separation of internal and external magnetic field contributions.

Importantly, the present study does not attempt to identify individual pre-earthquake geomagnetic anomalies or to establish a one-to-one correspondence between geomagnetic signals and earthquakes. Geomagnetic anomalies may occur without a subsequent earthquake, and earthquakes may occur without identifiable preceding geomagnetic anomalies. The analysis instead compares annual regression slopes of the

total geomagnetic field intensity with annual cumulative seismic energy. It is therefore exploratory and does not establish earthquake precursors or a causal relationship.

The annual regression slopes obtained using the complete, filtered, and quiet-day datasets are presented in Table 2. The pooled regression results for the entire 2021–2025 period, together with the corresponding numbers of daily observations, are presented in Table 3. The comparison shows that excluding days with daily maximum Kp ≥ 5 results in only small changes in the pooled regression slopes, approximately 0.4–1.0% across the five observatories. The quiet-day slopes are also broadly comparable with those obtained from the complete dataset, although somewhat larger differences are observed at certain stations and years. These findings indicate that the estimated long-term trends are generally not strongly affected by the inclusion of days with elevated geomagnetic activity. However, the possible influence of external magnetic field variations, particularly at JAI, cannot be completely excluded.

Table 2. Annual regression slopes (nT/day)

Observatory	Subset	2021	2022	2023	2024	2025
ART	All days	0.2514	0.2239	0.2084	0.2180	0.1980
	Excl. Kp ≥ 5	0.2504	0.2260	0.2117	0.2234	0.1980
	Quiet (Kp ≤ 2)	0.2457	0.2216	0.1994	0.2336	0.2070
IZN	All days	0.1912	0.1767	0.1522	0.1352	0.1085
	Excl. Kp ≥ 5	0.1914	0.1769	0.1517	0.1354	0.1080
	Quiet (Kp ≤ 2)	0.1920	0.1760	0.1518	0.1371	0.1165
JAI	All days	0.2370	0.1294	0.0934	0.0863	0.0959
	Excl. Kp ≥ 5	0.2376	0.1283	0.0936	0.0861	0.0960
	Quiet (Kp ≤ 2)	0.2415	0.1212	0.0727	0.0876	0.1039
NVS	All days	0.2161	0.2015	0.1929	0.2029	0.1722
	Excl. Kp ≥ 5	0.2172	0.2016	0.1927	0.2058	0.1708
	Quiet (Kp ≤ 2)	0.2174	0.1936	0.1768	0.2128	0.1786
YNBZ	All days	0.1722	0.1968	0.1733	0.1671	0.1461
	Excl. Kp ≥ 5	0.1726	0.1968	0.1744	0.1685	0.1491
	Quiet (Kp ≤ 2)	0.1843	0.1976	0.1705	0.1713	0.1404

Note: Slopes were calculated by regressing daily mean values against day number. "Excl. Kp ≥ 5" excludes days with a daily maximum Kp index ≥ 5. "Quiet" includes days for which all eight 3-hourly Kp values were ≤ 2. YNBZ data start on 25 June 2021.

Table 3. Pooled 2021–2025 regression slopes (nT/day); number of observations in parentheses

Observatory	All days	Excluding Kp ≥ 5 days	Quiet days (Kp ≤ 2)	Kp ≥ 5 days only
ART	0.2126 (1501)	0.2147 (1344)	0.2180 (342)	0.2025 (157)
IZN	0.1328 (1698)	0.1334 (1516)	0.1426 (385)	0.1242 (182)
JAI	0.1225 (1779)	0.1230 (1593)	0.1328 (414)	0.1160 (186)
NVS	0.1916 (1809)	0.1928 (1618)	0.1954 (424)	0.1863 (191)
YNBZ	0.1696 (1585)	0.1707 (1409)	0.1733 (334)	0.1660 (176)

Note: Kp index data were obtained from GFZ Potsdam. The values in parentheses indicate the number of daily observations used in each regression. Detailed statistical results, including sample size, standard errors, and coefficients of determination (R^2), are provided in Supplementary Table S1.

2.4. Linear Regression Analysis

To quantify the temporal rate of change in the total geomagnetic field intensity (T), Ordinary Least Squares (OLS) linear regression was applied [8].

The regression analysis was performed separately for each calendar year at each observatory. Daily mean values of the total geomagnetic field intensity (T), derived from the original one-minute INTERMAGNET observations, were used as the dependent variable, while the corresponding day number within the year was used as the independent variable.

Only days with available daily mean values were included in the analysis. Missing days were neither interpolated nor replaced, and duplicate records and entries with missing values were excluded. Consequently, the number of valid daily observations (N) varied among observatories and years. The annual observation counts are summarized in Table 4.

The slope of the fitted regression line represents the rate of change in the total geomagnetic field intensity, expressed in nT/day. For comparison, the daily slope was converted into an annualized rate (nT/year) by multiplying it by 365, corresponding to a standardized 365-day year.

It should be noted that the estimated trends represent changes in the observed total geomagnetic field intensity and may include contributions from both internal and external geomagnetic field sources. The potential influence of geomagnetic disturbances was therefore evaluated separately using the planetary Kp index, as described in Section 2.3. Conceptually, the observed intensity can be written as an approximate scalar sum, $T_{obs}(t) \approx T_{core}(t) + T_{lith} + T_{ext}(t) + T_{ind}(t) + \varepsilon(t)$, where the terms denote the core, lithospheric, external (ionospheric–magnetospheric) and induced contributions and the measurement noise [26]. A rigorous separation requires vector-field modelling; the fitted slope b should therefore be read as the combined rate of change of all these terms, not as the core contribution alone.

The regression model is expressed as: $$T = a + bt \quad (1)$$

- T – total geomagnetic field intensity (nT; daily mean value);
- t – time (days; day number within the calendar year, 1 January = 0);
- a – regression intercept (nT), representing the estimated value of the geomagnetic field intensity at t = 0;
- b – regression slope (nT/day), representing the rate of change of the geomagnetic field intensity with time.

The regression slope was calculated using the following formula:

Where: $$b = \frac{n\sum xy - \sum x \sum y}{n\sum x^2 - (\sum x)^2} \quad (2)$$

- n is the number of observations,
- x is the observation time t (days),
- y is the total geomagnetic field intensity T (nT).

Table 4. Number of valid daily mean geomagnetic field observations (N) used in the annual linear regression analysis for each observatory during 2021–2025

Observatory	2021	2022	2023	2024	2025
ART	199	348	247	346	361
IZN	318	337	352	341	350
JAI	351	347	353	363	365
NVS	363	362	360	361	363
YNBZ	181	312	365	364	363

The regression slope (2) represents the average rate of temporal change in the total geomagnetic field intensity. A positive slope indicates an increasing trend in the geomagnetic field intensity over time, whereas a negative slope indicates a decreasing trend. The statistical significance of the regression results was evaluated based on p-values, according to the criteria presented in Table 5.

Table 5. Interpretation of p-values used for statistical significance assessment

p-value	Statistical interpretation
$p < 0.05$	Statistically significant; the regression slope differs significantly from zero.
$p < 0.01$	Highly statistically significant.
$p < 0.001$	Very highly statistically significant (nominal p-value; see the note on autocorrelation in Section 2.4).
$p > 0.05$	Not statistically significant; there is insufficient evidence to conclude that the regression slope differs from zero.

Daily mean values were regressed against the day number within each calendar year (1 January = day 0), so that missing days do not distort the time axis. Slopes obtained in nT/day were converted to annual rates by multiplying by 365 (nT/year = nT/day × 365); the same factor was used for all observatories and years (using 365.25, or 366 for the leap year 2024, changes the values by less than 0.3%). Because each regression uses the daily values of a single calendar year, the slope describes the within-year rate of change of the total field, which contains the secular variation of the internal field together with seasonal and external-field contributions. To check whether the within-year slopes can be used as a proxy for the secular variation rate, they were compared with the year-to-year changes of the annual mean values (Section 3.1, Table 8). Consecutive daily values are autocorrelated (the lag-1 autocorrelation of the regression residuals ranged from about -0.03 to 0.95, being highest at JAI), so the nominal p-values overstate the statistical significance and are used here only descriptively. Autocorrelation-robust (heteroskedasticity- and autocorrelation-consistent) covariance estimators [29] and the inclusion of annual and semi-annual harmonic terms [28] would provide more realistic uncertainties for the slopes; for longer records, Singular Spectrum Analysis [30] could be used to separate the long-term trend from oscillatory components. These refinements are beyond the scope of the present descriptive analysis.

2.5. Spatial Mapping of Regression Slopes

The annual regression slope values (nT/year) calculated for each geomagnetic observatory were imported into ArcGIS 10.8 to examine their spatial distribution. The geographic coordinates (latitude and longitude) of each observatory were associated with the corresponding annual regression slope values for the period 2021–2025.

The Inverse Distance Weighting (IDW) interpolation method was applied to generate spatial distribution surfaces from the observatory-based regression slope values. IDW is a deterministic interpolation technique in which estimated values at unsampled locations are calculated as weighted averages of nearby observations. The weights are assigned according to the inverse of the distance between the estimation location and the measured points, meaning that observations closer to the estimation location have a greater influence on the interpolated value [22].

To ensure consistency and comparability among the annual maps, identical interpolation settings, coordinate reference system, spatial extent, and output raster cell size were maintained for all maps covering the 2021–2025 study period.

The interpolation was performed using the IDW tool in ArcGIS 10.8 with a power parameter of 2, a variable search radius, and five neighboring points. Since the analysis included only five observatories, all

available observatory points contributed to each interpolated cell. Consequently, the interpolation effectively represents a global IDW approach. The output raster cell size was 0.118052 decimal degrees, and the geographic coordinates were defined using the WGS 1984 coordinate reference system.

To assess interpolation accuracy, leave-one-out cross-validation (LOOCV) was applied. In this procedure, each observatory was omitted in turn, and its regression slope was predicted using the remaining four observatories with the IDW method (power = 2). Distances were calculated using geographic coordinates in degrees. The root mean square error (RMSE) ranged from 13.9 to 20.1 nT/year across the five annual interpolation maps, with a mean RMSE of 16.8 nT/year. These errors were comparable to the standard deviations of the regression slopes among the observatories, which ranged from 11.8 to 19.4 nT/year. These results indicate that the predictive accuracy of the IDW interpolation is limited by the small number of available observatories. Satellite-derived geomagnetic virtual observatories and their secular variation products [3] could provide additional spatial constraints beyond the five observatories used here.

It should also be noted that interpolation was performed using geographic coordinates rather than geomagnetic coordinates. Geographic coordinates were retained to represent the actual geographical distribution of the observatories and to maintain consistency with the geographic study area. However, this approach does not explicitly account for variations in geomagnetic latitude or geomagnetic field geometry. In particular, the low-latitude station JAI may be influenced by external current systems, including the equatorial electrojet (EEJ), whose effects are not represented by geographic distance-based interpolation.

Furthermore, IDW is a distance-based interpolation method and does not explicitly incorporate the physical processes governing geomagnetic field variations. The use of geographic coordinates also means that the distances used in the interpolation are not expressed as uniform physical distances across the study area. Therefore, the resulting maps should be interpreted as approximate spatial representations of the annual regression slopes rather than as a physical model or definitive representation of geomagnetic secular variation across the entire study region.

2.6. Comparison of Geomagnetic Regression Slopes and Seismic Energy

To investigate the possible temporal relationship between geomagnetic secular variation and regional seismic activity, the annual regression slope (nT/year) of the total geomagnetic field intensity (T) was compared with the annual cumulative seismic energy for each observatory.

Earthquake data for the period 2021–2025 were obtained from the European-Mediterranean Seismological Centre (EMSC) earthquake catalogue [21]. For each geomagnetic observatory, earthquakes with a magnitude of $M \geq 4.0$ occurring within a 200-km radius of the observatory were selected. The magnitude threshold of $M \geq 4.0$ was adopted based on previous studies investigating the relationship between geomagnetic variations and seismic energy release. For example, Chen et al. analyzed earthquakes with magnitudes greater than 4.0 within a 150-km radius of the Lunping Geomagnetic Observatory and examined their cumulative seismic energy release in relation to geomagnetic transfer function variations [23]. Following this approach, the present study uses $M \geq 4.0$ as an operational selection criterion to focus on moderate and larger earthquakes contributing to regional seismic energy release.

The seismic energy of each earthquake was calculated using the Gutenberg–Richter relationship [9]:

$$log_{10}E = 1.5M + 4.8 \quad (3)$$

where **E** is the seismic energy (**J**) and **M** is the earthquake magnitude.

The seismic energies of all selected earthquakes occurring within each calendar year were summed to obtain the annual cumulative seismic energy for each observatory. These annual energy values were then compared with the corresponding annual regression slopes (nT/year) of the total geomagnetic field intensity. The 200-km radius and the $M \geq 4.0$ threshold were not tested for sensitivity, and the EMSC catalogue may combine different magnitude types, to which Eq. (3) was applied without harmonisation. Annual totals can also be dominated by a single event: by Eq. (3), one M 5.0 earthquake releases about 2×10^{12} J, comparable to the largest annual values in Table 9. The annual energy should therefore be read together with the number and magnitude distribution of the events.

Because only five annual observations (2021–2025) were available for each observatory, the analysis was intended to identify possible temporal similarities between the two datasets. Therefore, the results should be interpreted as a comparative trend analysis rather than evidence of a direct causal relationship between seismic activity and geomagnetic secular variation.

3. Results and Discussion

3.1. Regression analysis of the total geomagnetic field intensity

To quantitatively evaluate the long-term variation of the geomagnetic field, linear regression analysis was performed using the daily mean values of the total geomagnetic field intensity (T) for each observatory during the period 2021–2025. The regression slope (nT/year) was adopted as the primary indicator of the annual rate of change of the field, which is used here as a proxy for the secular variation rate (see Table 11 and Section 2.4 for the supporting comparison). To assess the reliability and statistical significance of the regression models, the number of observations (n), coefficient of determination (R^2), and p-value were calculated for each observatory and each year. The regression analysis was performed using Equations (1) and (2), and the resulting regression statistics are summarized in Tables 6–10.

Table 6. Linear regression results for the IZN Observatory (2021–2025)

Year	Available days (n)	Regression Slope (nT/day)	Regression Slope (nT/year)	R^2	p-value
2021	318	0.191232	69.800	0.9877	<0.001
2022	337	0.176702	64.496	0.9794	<0.001
2023	352	0.152189	55.549	0.9409	<0.001
2024	341	0.135151	49.330	0.8793	<0.001
2025	350	0.108519	39.609	0.9177	<0.001

According to Table 6, the regression analysis of the daily mean values of the total geomagnetic field intensity (T) at the IZN Observatory during 2021–2025 revealed a positive trend in all years. The regression slope gradually decreased from 69.80 nT/year in 2021 to 39.61 nT/year in 2025. This indicates that although the total geomagnetic field intensity continued to increase, its rate of increase progressively declined over the study period. The high coefficients of determination (R^2 = 0.879–0.988) demonstrate that the linear regression model provided an excellent fit to the observed temporal variations. Furthermore, all regression models were statistically significant ($p < 0.001$), indicating statistically significant trends (nominal p-values; see Section 2.4).

Table 7. Linear regression results for the JAI Observatory (2021–2025)

Year	Available days (n)	Slope (nT/day)	Slope (nT/year)	R^2	p-value
2021	351	0.2370	86.51	0.9822	<0.001
2022	347	0.1294	47.23	0.8474	<0.001
2023	353	0.0934	34.11	0.7924	<0.001
2024	363	0.0863	31.48	0.7272	<0.001
2025	365	0.0959	34.99	0.9165	<0.001

According to Table 7, the regression analysis of the daily mean values of the total geomagnetic field intensity (T) at the JAI Observatory during 2021–2025 revealed a positive linear trend in all years. The regression slope decreased markedly from 86.51 nT/year in 2021 to 31.48 nT/year in 2024, followed by a slight increase to 34.99 nT/year in 2025. These results indicate that although the total geomagnetic field intensity continued to increase throughout the study period, its rate of increase declined after 2021 and became relatively stable during 2024–2025. The coefficients of determination (R^2 = 0.727–0.982) indicate that the linear regression models adequately described the observed temporal variations. Furthermore, all regression models were statistically significant ($p < 0.001$), indicating statistically significant trends (nominal p-values; see Section 2.4).

Table 8. Linear regression results for the NVS Observatory (2021–2025)

Year	Available days (n)	Slope (nT/day)	Slope (nT/year)	R^2	p-value
2021	363	0.2161	78.88	0.9524	<0.001
2022	362	0.2015	73.55	0.9109	<0.001
2023	360	0.1929	70.41	0.8290	<0.001
2024	361	0.2029	74.05	0.8714	<0.001
2025	363	0.1722	62.84	0.7409	<0.001

According to Table 8, the regression analysis of the daily mean values of the total geomagnetic field intensity (T) at the NVS Observatory during 2021–2025 revealed a positive linear trend in all years. The regression slope generally decreased from 78.88 nT/year in 2021 to 62.84 nT/year in 2025. These results indicate that although the total geomagnetic field intensity continued to increase throughout the study period, its rate of increase gradually declined over time. The coefficients of determination (R^2 = 0.741–0.952) indicate that the linear regression models adequately described the observed temporal variations. Furthermore, all regression models were statistically significant ($p< 0.001$), indicating statistically significant trends (nominal p-values; see Section 2.4).

Table 9. Linear regression results for the YNBZ Observatory (2021–2025)

Year	Available days (n)	Slope (nT/day)	Slope (nT/year)	R^2	p-value
2021	181	0.1722	62.85	0.911	<0.001
2022	312	0.1968	71.83	0.957	<0.001
2023	365	0.1733	63.24	0.908	<0.001
2024	364	0.1671	60.99	0.914	<0.001
2025	363	0.1461	53.32	0.855	<0.001

According to Table 9, the regression analysis of the daily mean values of the total geomagnetic field intensity (T) at the Yangibozor (YNBZ) Observatory during 2021–2025 revealed a positive linear trend in all years. The regression slope reached its highest value in 2022 (71.83 nT/year) and then gradually decreased to 53.32 nT/year in 2025. These results indicate that although the total geomagnetic field intensity continued to increase throughout the study period, its rate of increase gradually declined after 2022. The coefficients of determination (R^2 = 0.855–0.957) indicate that the linear regression models provided an excellent fit to the observed temporal variations. Furthermore, all regression models were statistically significant ($p < 0.001$), indicating statistically significant trends (nominal p-values; see Section 2.4).

Table 10. Linear regression results for the ART Observatory (2021–2025)

Year	Available days (n)	Slope (nT/day)	Slope (nT/year)	R^2	p-value
2021	199	0.2514	91.76	0.837	<0.001
2022	348	0.2239	81.73	0.864	<0.001
2023	247	0.2084	76.05	0.769	<0.001
2024	346	0.2180	79.55	0.797	<0.001
2025	361	0.1980	72.25	0.600	<0.001

According to Table 10, the regression analysis of the daily mean values of the total geomagnetic field intensity (T) at the ART Observatory during 2021–2025 revealed a positive linear trend in all years. The regression slope generally decreased from 91.76 nT/year in 2021 to 72.25 nT/year in 2025, indicating an overall declining trend in the rate of geomagnetic field change. However, a slight increase was observed in 2024 (79.55 nT/year) compared with 2023 (76.05 nT/year). These results indicate that although the total geomagnetic field intensity continued to increase throughout the study period, its rate of increase gradually declined over time. The coefficients of determination (R^2 = 0.600–0.864) indicate that the linear regression models adequately described the observed temporal variations. Furthermore, all regression models were statistically significant ($p < 0.001$), indicating statistically significant trends (nominal p-values; see Section 2.4).

Table 11. Year-to-year change of the annual mean total field (Δ annual mean) compared with the average of the two corresponding annual regression slopes (mean slope = slope × 365, nT/year). * The 2021 annual mean is based on a partial year (ART: 1 January–20 July; YNBZ: from 25 June).

Years	ART Δ annual mean (nT/year)	ART mean slope (nT/year)	IZN Δ annual mean (nT/year)	IZN mean slope (nT/year)	NVS Δ annual mean (nT/year)	NVS mean slope (nT/year)	JAI Δ annual mean (nT/year)	JAI mean slope (nT/year)	YNBZ Δ annual mean (nT/year)	YNBZ mean slope (nT/year)
2021–22	102.8*	86.7	69.4	67.1	76.6	76.2	75.4	66.9	53.9*	67.3
2022–23	88.4	78.9	61.6	60.0	70.9	72.0	45.0	40.7	62.6	67.5
2023–24	68.0	77.8	23.2	52.4	68.6	72.2	31.4	32.8	62.2	62.1
2024–25	70.7	75.9	44.1	44.5	63.7	68.4	33.4	33.2	56.3	57.2

To check whether the within-year regression slopes can be used as a proxy for the secular variation rate, they were compared with the year-to-year change of the annual mean total field (Table 11). For each pair of consecutive years, the change of the annual mean (Δ) was compared with the average of the two corresponding annual slopes (slope × 365). The two estimates agree within 10 nT/year in 17 of the 20

comparisons. The exceptions are the 2021–2022 pairs at ART and YNBZ, where the 2021 annual mean is based on a partial year, and IZN in 2023–2024 (Δ = 23.2 nT/year against 52.4 nT/year from the slopes). This agreement supports the use of the annual regression slopes as an approximate indicator of the year-to-year field change; however, seasonal and external-field contributions cannot be excluded, particularly where the record is incomplete.

Table 10. Observed annual regression slopes and the change of total intensity over each calendar year predicted by IGRF-14 at the observatory coordinates (nT/year); residual = observed − IGRF-14.

Observatory	Quantity	2021	2022	2023	2024	2025	Mean
ART	Observed slope	91.8	81.7	76.0	79.5	72.2	80.3
	IGRF-14	71.9	71.9	71.9	72.1	68.5	71.3
	Residual	+19.9	+9.8	+4.1	+7.4	+3.7	+9.0
NVS	Observed slope	78.9	73.5	70.4	74.0	62.8	71.9
	IGRF-14	61.0	61.1	61.1	61.3	58.7	60.6
	Residual	+17.8	+12.5	+9.3	+12.7	+4.2	+11.3
YNBZ	Observed slope	62.9	71.8	63.2	61.0	53.3	62.4
	IGRF-14	69.5	69.5	69.5	69.7	62.1	68.1
	Residual	−6.6	+2.3	−6.3	−8.7	−8.8	−5.6
IZN	Observed slope	69.8	64.5	55.5	49.3	39.6	55.8
	IGRF-14	57.4	57.4	57.4	57.6	50.0	56.0
	Residual	+12.4	+7.1	−1.9	−8.3	−10.4	−0.2
JAI	Observed slope	86.5	47.2	34.1	31.5	35.0	46.9
	IGRF-14	58.5	58.5	58.6	58.8	44.1	55.7
	Residual	+28.0	−11.3	−24.5	−27.3	−9.1	−8.8

3.2. Comparison between the regression slope of the total geomagnetic field intensity and annual seismic energy

During the period 2021–2025, the annual regression slopes (nT/year) of the total geomagnetic field intensity (T) were estimated for the ART, IZN, JAI, NVS, and Yangibozor (YNBZ) geomagnetic observatories. To investigate the possible relationship between geomagnetic secular variation and regional seismic activity, the annual regression slope values were compared with the annual cumulative seismic energy released by earthquakes of magnitude M ≥ 4.0 occurring within a 200-km radius of each observatory (Table 12).

Table 12. Annual regression slope of the total geomagnetic field intensity and annual seismic energy within a 200 km radius around the selected geomagnetic observatories (2021–2025)

Year	ART Slope (nT/year)	ART Energy (J)	IZN Slope (nT/year)	IZN Energy (J)	NVS Slope (nT/year)	NVS Energy (J)	JAI Slope (nT/year)	JAI Energy (J)	YNBZ Slope (nT/year)	YNBZ Energy (J)
2021	91.76	0	69.80	7.29×10^{11}	78.88	1.33×10^{11}	86.51	0	62.85	4.68×10^{11}
2022	81.73	2.40×10^{11}	64.50	6.19×10^{12}	73.55	0	47.23	0	71.83	2.66×10^{11}
2023	76.05	8.90×10^{10}	55.55	6.52×10^{11}	70.41	4.17×10^{11}	34.11	1.80×10^{11}	63.24	3.57×10^{11}
2024	79.55	4.50×10^{10}	49.33	2.32×10^{11}	74.05	7.10×10^{11}	31.48	9.96×10^{10}	60.99	1.97×10^{11}
2025	72.25	0	39.61	2.62×10^{12}	62.84	6.30×10^{10}	34.99	2.44×10^{11}	53.32	1.03×10^{12}

The comparison between annual geomagnetic regression slopes and cumulative seismic energy revealed considerable differences among the observatories. No consistent relationship was observed across all study sites. For each observatory, annual seismic energy was calculated using earthquakes with magnitudes of M ≥ 4.0 occurring within a 200-km radius. No earthquakes meeting this criterion occurred within a 200-km radius

of the JAI Observatory in 2021–2022, the ART Observatory in 2021 and 2025, or the NVS Observatory in 2022. Accordingly, the annual seismic energy for these years was considered zero (Table 12).

At the Yangibozor (YNBZ) Observatory, the annual regression slope reached its maximum value in 2022 (71.83 nT/year), while the annual seismic energy remained relatively low. In contrast, in 2025, the regression slope decreased to its minimum value (53.32 nT/year), whereas the annual seismic energy reached its maximum (1.03×10^{12} J). This temporal pattern suggests an inverse variation between the two parameters during these years. However, the limited number of annual observations does not allow this pattern to be considered evidence of a statistically established relationship.

At the IZN Observatory, annual seismic energy peaked in 2022 and 2025, while the geomagnetic regression slope generally decreased throughout the study period, from 69.80 to 39.61 nT/year. Nevertheless, the temporal variations of these parameters did not demonstrate a consistent pattern of correspondence.

The NVS and ART observatories also exhibited differences in the temporal behavior of geomagnetic regression slopes and annual seismic energy. At the JAI Observatory, the comparison was limited to three annual observations (2023–2025), because no qualifying earthquakes occurred during 2021–2022. Overall, these comparisons provide a preliminary descriptive assessment of the possible relationship between geomagnetic field variations and regional seismic energy release. Since the analysis is based on only 3–5 annual observations per observatory, no statistically reliable correlation or causal relationship can be established. Furthermore, the annual aggregation of daily geomagnetic measurements does not account for temporal autocorrelation. Therefore, time-series analyses using methods that explicitly account for autocorrelation are needed to investigate this relationship more rigorously. For orientation, with $n = 5$ even a correlation coefficient of $r = 0$ has a 95% confidence interval of about −0.88 to +0.88 (Fisher transformation), and for $n = 3$ (JAI) the interval cannot be defined; correlation coefficients are therefore not reported.

Overall, the results suggest that the temporal relationship between geomagnetic secular variation and regional seismic energy is site-dependent rather than universal. Different observatories exhibited inverse (YNBZ), positive (NVS and ART), negligible (IZN), or uncertain (JAI) relationships. Because only five or fewer annual observations were available for each observatory, these findings should be considered preliminary and do not demonstrate a causal relationship. Longer observation periods and a larger number of geomagnetic observatories are required to evaluate these relationships more reliably.

The present results are generally consistent with the findings of Arora and Singh, who suggested that the relationship between local geomagnetic anomalies and seismic activity may only be observable in certain tectonically active regions [10]. They are also in agreement with the recent review by Winata et al., which concluded that the relationship between geomagnetic anomalies and earthquakes remains inconclusive and requires further investigation [11]. Further work could also compare geomagnetic residuals and regional seismicity with other Earth-dynamics observables, such as length-of-day and polar motion [28, 31], using temporal coherence analysis rather than linear trends alone.

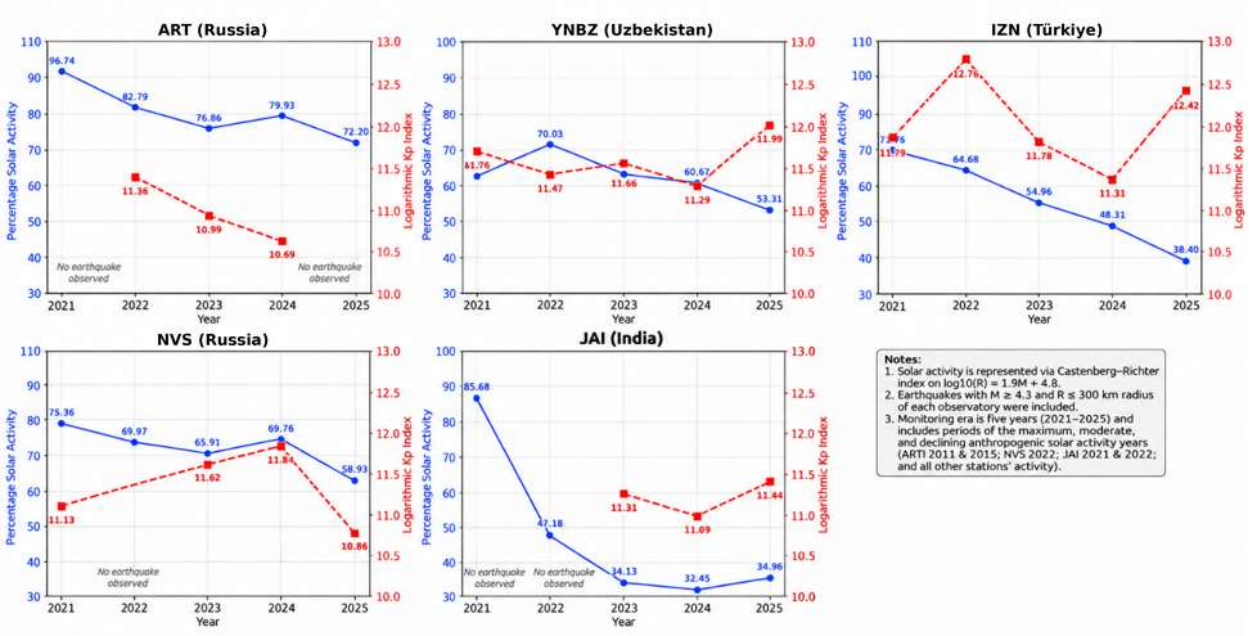

Figure 2. Annual variation of the regression slope of the total geomagnetic field intensity and $\log_{10}$(annual seismic energy) at the selected geomagnetic observatories during 2021–2025.

3.3. Spatiotemporal variation of regression slopes

To examine the spatial and temporal characteristics of the annual rate of change of the total geomagnetic field intensity, the annual regression slopes (nT/year) calculated for each observatory were interpolated with the IDW method in ArcGIS to produce distribution maps for 2021–2025 (Figures 3–7). Because the slopes are expressed in physical units (nT/year), they allow a quantitative comparison among observatories and between years. The within-year slopes are consistent with the year-to-year differences of the annual mean values (Table 11), which supports their use as a proxy for the secular variation rate; however, they may still contain seasonal and external-field contributions (Section 2.3). Because only five observatories are available and the cross-validation errors are comparable to the differences among the stations (Section 2.5), the maps indicate regional tendencies only and should not be regarded as a precise representation of the spatial distribution of secular variation.

It should be noted that the annual regression slopes estimated from daily mean geomagnetic field intensity values may reflect a combination of internal and external magnetic field contributions. Verbanac et al. [26] demonstrated that magnetospheric and ionospheric current systems can contribute to geomagnetic observatory annual means, even after temporal averaging. Furthermore, geomagnetic variations during magnetically quiet periods may still contain contributions from solar quiet (Sq) currents, particularly at low- and mid-latitude observatories. Therefore, although the Kp-based sensitivity analysis performed in this study helps assess the influence of geomagnetic disturbances, it does not completely eliminate all external field contributions. Consequently, the estimated regression slopes are interpreted as observed annual trends in total geomagnetic field intensity rather than as direct measurements of the secular variation of the Earth's internal magnetic field.

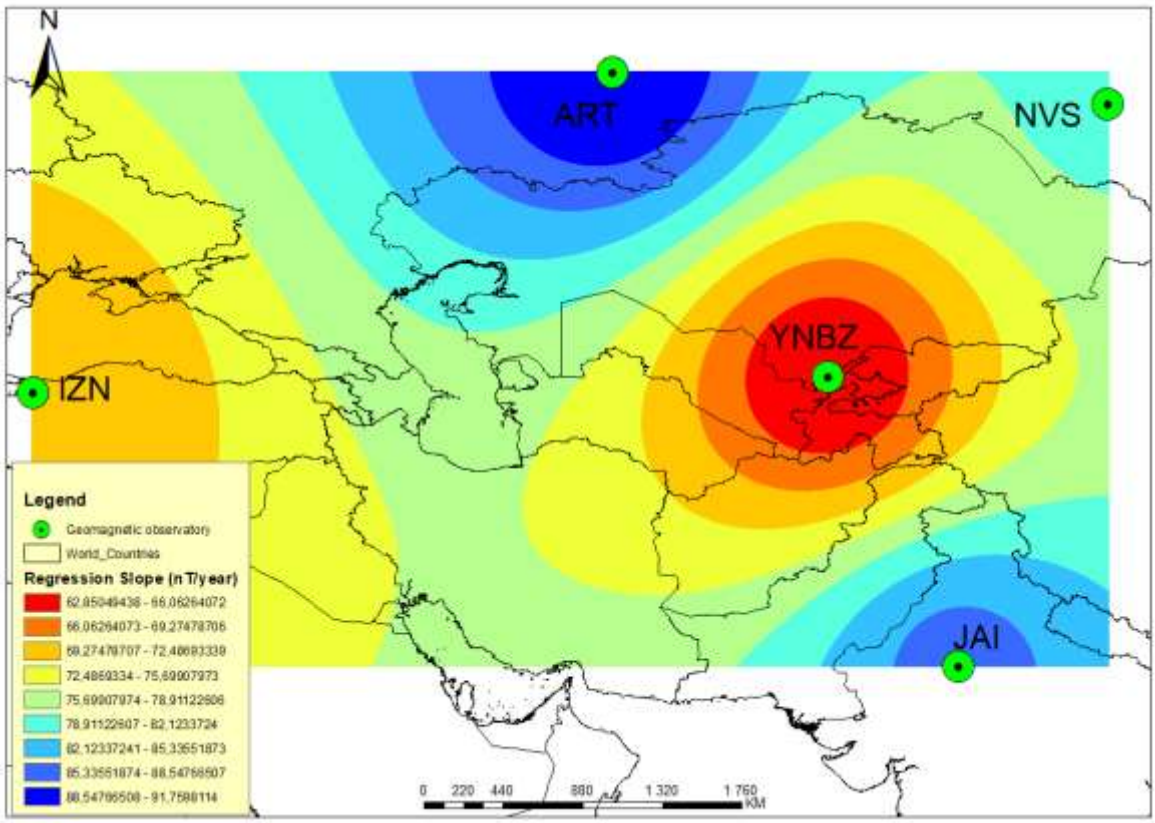

Figure 3. Spatial distribution of the regression slope of the total geomagnetic field intensity in 2021.

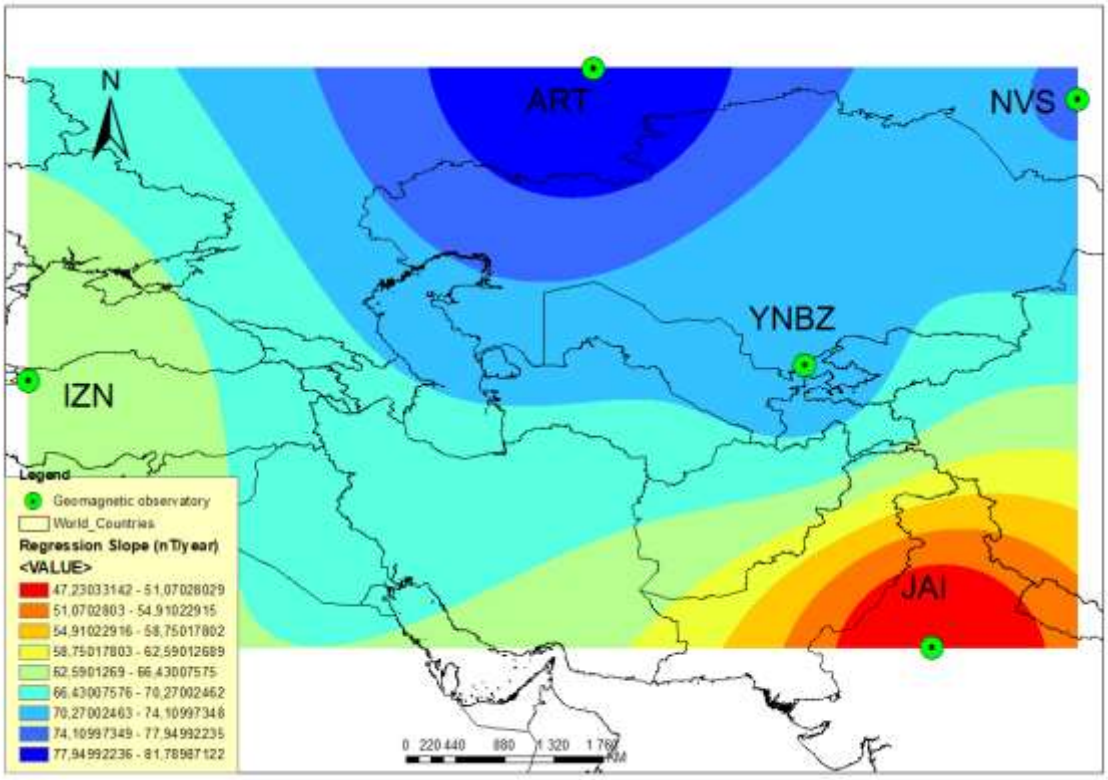

Figure 4. Spatial distribution of the regression slope of the total geomagnetic field intensity in 2022.

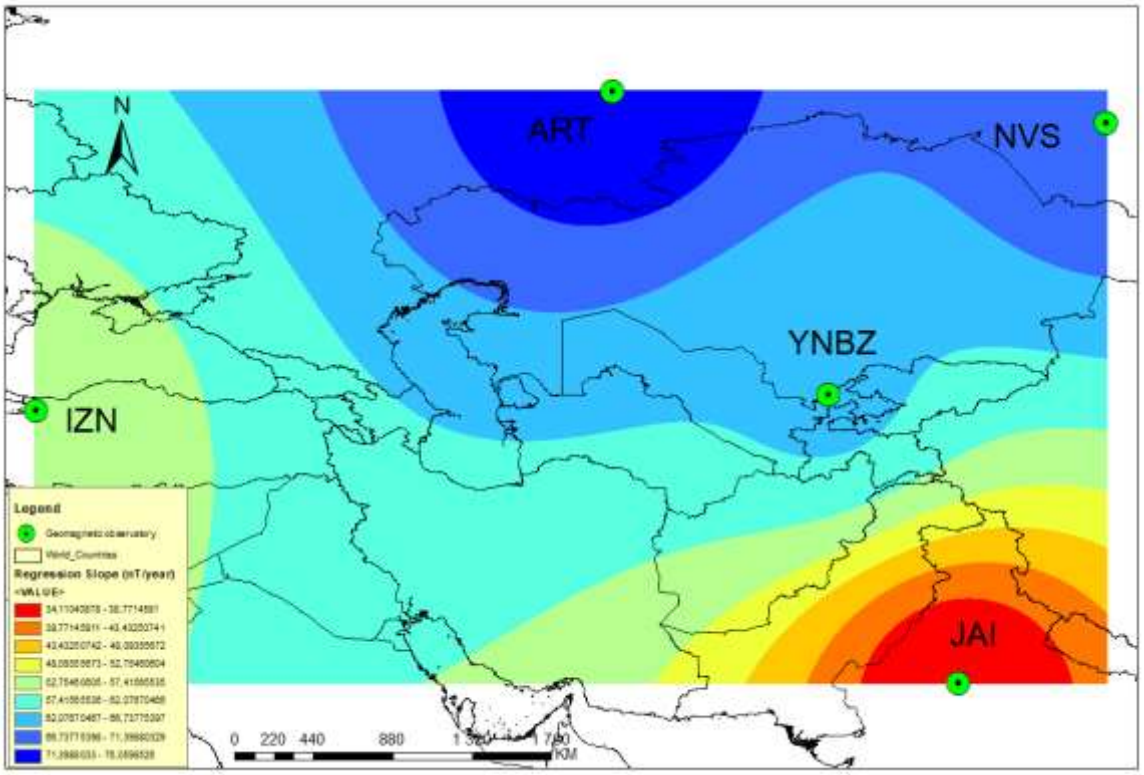

Figure 5. Spatial distribution of the regression slope of the total geomagnetic field intensity in 2023.

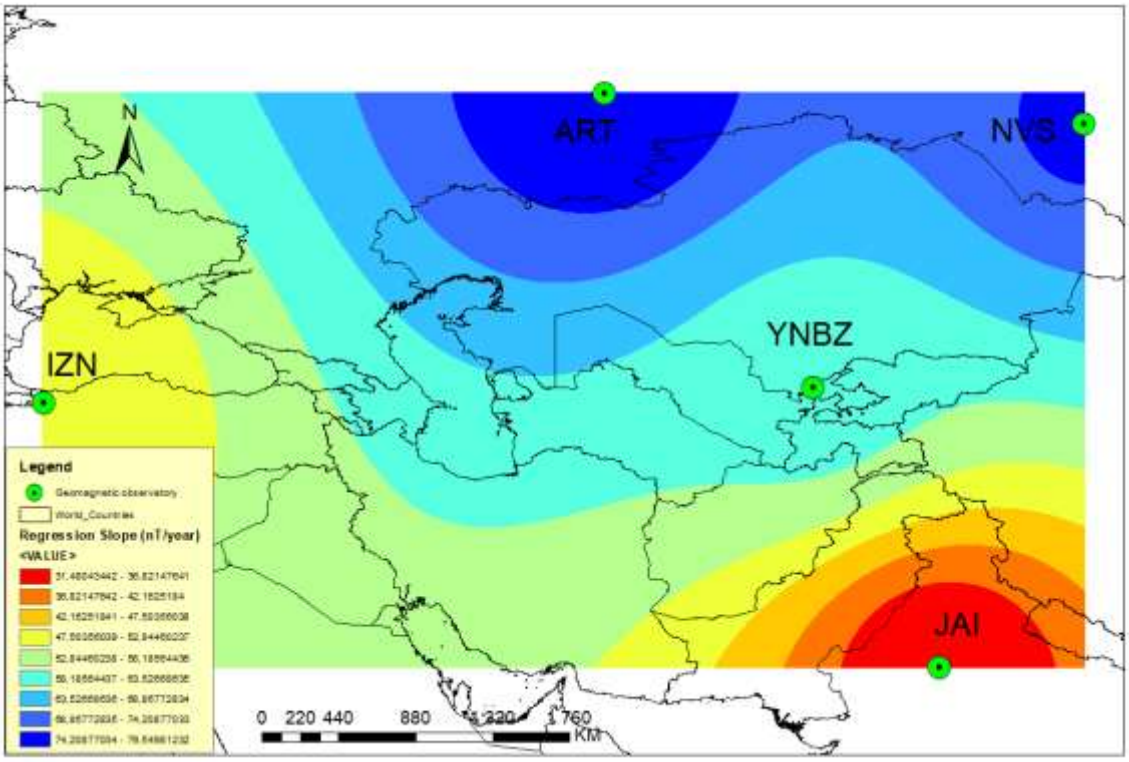

Figure 6. Spatial distribution of the regression slope of the total geomagnetic field intensity in 2024.

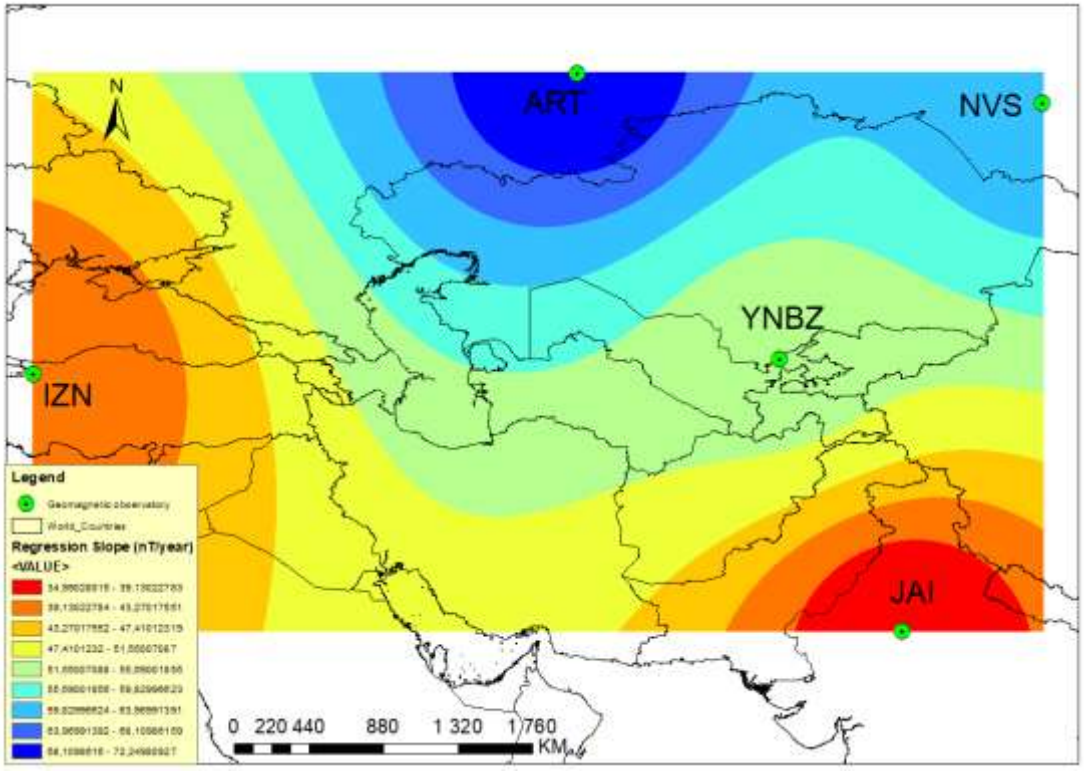

Figure 7. Spatial distribution of the regression slope of the total geomagnetic field intensity in 2025.

Figures 3–7 present the spatial distribution maps of the annual regression slopes (nT/year) of the total geomagnetic field intensity (T) for the five geomagnetic observatories during 2021–2025. The maps demonstrate that the rate of long-term geomagnetic field change was spatially heterogeneous across the study region. During the first years of the study, the highest regression slopes were observed at the ART and JAI observatories, whereas relatively lower values occurred at Yangibozor (YNBZ) and IZN. A gradual decrease in regression slope was observed at most observatories throughout the study period, indicating a reduction in the rate of change of the total geomagnetic field intensity.

The observed spatial and temporal differences are consistent with the characteristics of geomagnetic secular variation, which primarily reflects fluid motions within the Earth's electrically conducting outer core. As noted by Dobrica et al. [12], secular variation originates from complex core dynamics and therefore does not evolve uniformly over the Earth's surface. Consequently, differences in regression slopes among observatories are expected and reflect regional manifestations of the global geomagnetic field.

Another process that may contribute to the spatial variability of regression slopes is the westward drift of the geomagnetic field. Wei and Xu [1] demonstrated that the gradual westward displacement of geomagnetic field features, driven by outer-core dynamics, modifies the spatial distribution of the main field and its secular variation. Such large-scale processes may partly explain the regional differences observed in this study.

The comparison between the annual cumulative seismic energy and the annual regression slopes indicated that similar temporal tendencies were observed only at some observatories. ART exhibited an overall decline in both seismic energy and regression slope during 2022–2025. At Yangibozor (YNBZ), the highest slope (2022) coincided with low seismic energy and the lowest slope (2025) with the highest seismic energy, i.e. an inverse tendency in these years, whereas at JAI the slope decreased markedly between 2021

and 2023 and remained nearly constant thereafter, without a consistent relation to seismic energy. In contrast, IZN displayed a continuous decrease in regression slope despite renewed increases in seismic energy during 2025. These observations suggest that although similar trends may occur locally, they are not consistent across all observatories.

Overall, the results indicate that no universal linear relationship exists between annual seismic energy and the long-term rate of change of the total geomagnetic field. The estimated rates represent the combined effects of internal and external magnetic-field sources and cannot be attributed uniquely to core geodynamo processes using the present dataset. Contributions from external fields and local lithospheric sources cannot be excluded. Arora and Singh [10] and Winata et al. [11] likewise emphasized that evidence for a direct relationship between geomagnetic anomalies and earthquakes remains limited and inconclusive.

The present results are also consistent with previous studies describing the origin of secular variation. Yanovsky [13] and Bullard [14] attributed long-term geomagnetic field changes to fluid motions within the Earth's outer core, whereas Alldredge [18] emphasized that regional differences observed among geomagnetic observatories reflect the spatial distribution of geomagnetic field sources. In addition, long-term geomagnetic observations remain essential for monitoring secular variation and validating global geomagnetic field models [15,16]. Regional investigations in Uzbekistan have likewise demonstrated the importance of continuous geomagnetic monitoring for evaluating spatial and temporal variations of the magnetic field [17].

Finally, although the main source of secular variation is internal to the Earth, external contributions from the ionosphere and magnetosphere may also influence long-term geomagnetic observations. For example, Jin et al. [19] reported significant long-term changes in the ionosphere–plasmasphere system based on GPS-derived total electron content (TEC), suggesting that external space-weather processes should also be considered when interpreting long-term geomagnetic observations.

Conclusions

In this study, the rate of change in the mean total geomagnetic field intensity (T) during 2021–2025 was investigated at the ART, NVS, IZN, JAI, and Yangibozor (YNBZ) geomagnetic observatories using regression slope (nT/year). Regression analysis and spatial distribution maps revealed clear spatial differences in the rate of geomagnetic field intensity change among the selected observatories.

The obtained results indicate that the annual rate of change of the total geomagnetic field intensity (a proxy for secular variation) is not spatially uniform across the five observatories. The spatial distribution and temporal evolution of the regression slopes may be associated with the Earth's core dynamics, including geodynamo processes generated by the motion of electrically conductive molten material in the outer core, as well as the long-term evolution of the main geomagnetic field.

During 2021–2025, a general decreasing trend in the regression slope was observed at most observatories, indicating that although the total geomagnetic field intensity continued to change, its rate of change gradually decreased over the study period. Relatively higher regression slopes were observed at the ART and JAI observatories, whereas lower values were recorded at the Yangibozor (YNBZ) and IZN observatories. These regional differences may be related to geomagnetic latitude, regional geomagnetic field configuration, and spatial variations in the flow of the Earth's outer core.

Comparison of the regression slopes with the annual seismic energy showed that no consistent linear relationship exists between the two parameters across all observatories. Nevertheless, similar temporal tendencies were observed at several stations. In ART, both the regression slope and annual seismic energy generally decreased during the study period. At Yangibozor (YNBZ), the highest slope (2022) coincided with

low seismic energy and the lowest slope (2025) with the highest seismic energy. At IZN, the decrease in annual seismic energy after 2022 was accompanied by a decrease in the regression slope, whereas in 2025 the seismic energy increased again while the regression slope continued to decline. At JAI, the slope decreased markedly from 2021 to 2023 and remained nearly constant during 2023–2025. These observations suggest that local similarities may occur during certain periods; however, they do not represent a general relationship between seismic activity and long-term geomagnetic field changes.

Overall, this study demonstrates that combining geomagnetic observatory data with regression analysis and spatial mapping provides a useful approach for describing regional differences in the annual rate of change of the total geomagnetic field intensity, although external-field contributions, the small number of observatories and the short five-year period limit the interpretation. Future studies should extend the observation period, include a larger number of observatories, and integrate independent datasets such as Swarm, CHAOS, GNSS, and InSAR to achieve a more comprehensive understanding of the mechanisms controlling long-term geomagnetic field variations. In addition, the residuals between the observed slopes and the IGRF-14 predictions (Table 10) indicate where regional variations not explained by global models might be sought; this requires a more rigorous separation of internal and external contributions, a comparison with CHAOS-7 [27], and an examination of the time series together with length-of-day and polar-motion records [28, 31].

References

1. Wei, Z.-G., & Xu, W.-Y. (2003). Westward drift in secular variation of the main geomagnetic field inferred from IGRF. Earth, Planets and Space, 55, 237–243. https://doi.org/10.1186/BF03351745
2. Goguitchaichvili, A., Hernández-Quintero, E., García-Ruiz, R., Kravchinsky, V., Cejudo, R., & Cifuentes, G. (2022). Secular variation of the Earth's magnetic field revealed by Mexican Geomagnetic Repeat Stations during the last two centuries. Journal of South American Earth Sciences, 113, 103652. https://doi.org/10.1016/j.jsames.2021.103652.
3. Hammer, M. D., Finlay, C. C., & Olsen, N. (2022). Secular variation signals in magnetic field gradient tensor elements derived from satellite-based geomagnetic virtual observatories. Geophysical Journal International, 229(3), 2096–2114. https://doi.org/10.1093/gji/ggac004
4. Lemgharbi, A., Hamoudi, M., Lesur, V., Mandea, M., Amezza, T., & Abtout, A. (2026). Geomagnetic field modelling and USTHB IGRF-14 candidates. Earth, Planets and Space, 78, Article 151. https://doi.org/10.1186/s40623-026-02479-8
5. Wardinski, I., Terra Nova, F., & Amit, H. (2026). Models and predictions of Earth's magnetic field based on geomagnetic observatory data. Earth, Planets and Space, 78, Article 101. https://doi.org/10.1186/s40623-026-02410-1
6. Beggan, C. D., Kloss, C., Amblard, P., Amezza, T., Amit, H., Aubert, J., Baerenzung, J., Bregnhøj Lauridsen, J., Brown, W., Califf, S., Campuzano, S. A., Chauvet, L., Chulliat, A., Claveau, R., Coïsson, P., da Silva, M., Davies, C., Deborde, R., Dobrovolsky, M., ... Zhou, B. (2026). International geomagnetic reference field: The fourteenth generation. Earth, Planets and Space, 78, Article 127. https://doi.org/10.1186/s40623-025-02360-0
7. Maksudov, S. X., Yusupov, V., Khakimov, E. N., Sagdullaeva, K. A., Shakhriyev, B. B., & Nazarov, S. (2025). The Manifestation of Local Anomalous Variations of the Geomagnetic Field in Uzbekistan in Connection With the Problem of Earthquake Forecasting. Russian Journal of Earth Sciences. https://doi.org/10.2205/2025es001037
8. Montgomery, D. C., Peck, E. A., & Vining, G. G. (2021). Introduction to Linear Regression Analysis (6th ed.). Wiley.
9. Gutenberg, B., & Richter, C. F. (1956). Magnitude and energy of earthquakes. Annali di Geofisica, 9, 1–15.
10. Arora, B. R., & Singh, B. P. (1979). Geomagnetic field precursors associated with earthquakes. Mausam, 30(2), 303–310. https://doi.org/10.54302/mausam.v30i2.3036
11. Winata, E. N., Rosid, M. S., & Febriani, F. (2025). Advances and challenges in the study of ULF geomagnetic anomalies for earthquake precursors: A four-decade critical literature review. Earthquake Research Advances, 5, Article 100438. https://doi.org/10.1016/j.eqrea.2025.100438
12. Dobrica, V., Demetrescu, C., & Stefan, C. (2013). Toward a better representation of the secular variation. Case study: The European network of geomagnetic observatories. Earth, Planets and Space, 65, 767–779.

https://doi.org/10.5047/eps.2012.12.001
13. Yanovsky, B. M. (1978). Earth's Magnetism. Leningrad: Leningrad University Press, 592 p. (in Russian).
14. Bullard, E. C. (1948). The secular change in the Earth's magnetic field. Geophysical Supplements to the Monthly Notices of the Royal Astronomical Society, 5(7), 248–257. https://doi.org/10.1111/j.1365-246X.1948.tb02940.x
15. Maksudov, S. Kh. (2024). On the study of anomalous variations of the geomagnetic field. Earthquake, 2(2). https://doi.org/10.59429/ear.v2i2.6826
16. Maksudov, S. Kh., Abdullabekov, K. N., & Tuichiev, A. I. (2021). Geomagnetic field variations caused by the processes occurring at different depths in the Earth's crust and upper mantle. Izvestiya, Physics of the Solid Earth, 57(3), 295–308. https://doi.org/10.1134/S1069351321020063
17. Yusupov, V. R., Shukurov, Z. F., & Yadigarov, E. M. (2021). Analysis of the geomagnetic field and vertical movement near the intersection of Karjantau and Tavaksay faults in Uzbekistan. Geodesy and Geodynamics, 12, 102–109. https://doi.org/10.1016/j.geog.2021.01.002
18. Alldredge, L. R. (1983). Varying geomagnetic anomalies and secular variation. Journal of Geophysical Research: Solid Earth, 88(B11), 9443–9451. https://doi.org/10.1029/JB088iB11p09443
19. Jin, S., Gao, C., Yuan, L., Guo, P., Calabia, A., Ruan, H., & Luo, P. (2021). Long-Term Variations of Plasmaspheric Total Electron Content from Topside GPS Observations on LEO Satellites. Remote Sensing, 13(4), 545. https://doi.org/10.3390/rs13040545
20. INTERMAGNET. INTERMAGNET Data Viewer. Available at: https://intermagnet.org (accessed January 2026).
21. European-Mediterranean Seismological Centre (EMSC). Earthquake Catalogue. Available at: https://www.emsc-csem.org (accessed January 2026).
22. Esri. ArcGIS Desktop 10.8 Documentation. Available at: https://desktop.arcgis.com (accessed January 2026).
23. Chen, K.-J., Chiu, B., & Lin, C.-H. (2006). A search for a correlation between time change in transfer functions and seismic energy release in northern Taiwan. Earth, Planets and Space, 58, 981–991. https://doi.org/10.1186/BF03351745
24. Mihai, A., Toader, V.-E., Moldovan, I.-A., & Radulian, M. (2023). Exploring the relationship between geomagnetic variations and seismic energy release in proximity to the Vrancea seismic zone. Atmosphere, 14(6), 1005. https://doi.org/10.3390/atmos14061005
25. Han, P., Hattori, K., Hirokawa, M., Zhuang, J., Chen, C.-H., Febriani, F., Yamaguchi, H., Yoshino, C., Liu, J.-Y., & Yoshida, S. (2014). Statistical analysis of ULF seismomagnetic phenomena at Kakioka, Japan, during 2001–2010. *Journal of Geophysical Research: Space Physics, 119*(6), 4998–5011. https://doi.org/10.1002/2014JA019789
26. Verbanac, G., Lühr, H., Rother, M., Korte, M., & Mandea, M. (2007). Contributions of the external field to the observatory annual means and a proposal for their corrections. Earth, Planets and Space, 59, 251–257. https://doi.org/10.1186/BF03353102
27. Finlay, C. C., Kloss, C., Olsen, N., Hammer, M. D., Tøffner-Clausen, L., Grayver, A., & Kuvshinov, A. (2020). The CHAOS-7 geomagnetic field model and observed changes in the South Atlantic Anomaly. *Earth, Planets and Space, 72*, 156. https://doi.org/10.1186/s40623-020-01252-9
28. Le Mouël, J.-L., Lopes, F., Courtillot, V., Gibert, D., & Boulé, J.-B. (2023). Is the Earth's Magnetic Field a Constant? A Legacy of Poisson. *Geosciences, 13*(7), 202. https://doi.org/10.3390/geosciences13070202
29. Newey, W. K., & West, K. D. (1987). A simple, positive semi-definite, heteroskedasticity and autocorrelation consistent covariance matrix. *Econometrica, 55*(3), 703–708. https://doi.org/10.2307/1913610
30. Vautard, R., & Ghil, M. (1989). Singular spectrum analysis in nonlinear dynamics, with applications to paleoclimatic time series. *Physica D: Nonlinear Phenomena, 35*(3), 395–424. https://doi.org/10.1016/0167-2789(89)90077-8
31. Dumont, S., de Bremond d'Ars, J., Boulé, J.-B., Courtillot, V., Gèze, M., Gibert, D., et al. (2025). On a planetary forcing of global seismicity. *Frontiers in Earth Science, 13*, 1587650. https://doi.org/10.3389/feart.2025.1587650